OPEN ACCESS

Saudi Journal of Oral and Dental Research
Abbreviated Key Title: Saudi J Oral Dent Res
ISSN 2518-1300 (Print) | ISSN 2518-1297 (Online)
Scholars Middle East Publishers, Dubai, United Arab Emirates
Journal homepage: https://saudijournals.com

Original Research Article **Radiology**

Anatomical Evaluation of the Greater Palatine Foramen: A Cone-Beam Computed Tomography Study in Tunisian Patients

Olfa Zaghden[1,2*], Nawres Ghadhab[1,2], Rym Kammoun[1,3,4], Sabra Jaafoura[5,6,7], Imen Chaabani[1,2], Touhami Ben Alaya[1,2]

[1]Department of Oral Radiology, University Dental Clinic, Monastir University, Monastir, Tunisia
[2]Research Laboratory "Bioactive Natural Substances and Biotechnology" (UR17ES49)
[3]Laboratory of Histology and Embryology, Faculty of Dental Medicine of Monastir, University of Monastir, Monastir, Tunisia
[4]ABCDF Laboratory for Biological Clinical and Dento-Facial Approach, University of Monastir, Monastir, Tunisia
[5]Department of Dental Biomaterials, Faculty of Dental Medicine of Monastir, University of Monastir, Monastir, Tunisia
[6]ABCDF Laboratory (LR12ES10), Faculty of Dental Medicine, University of Monastir, Monastir, Tunisia
[7]Natural Substances Laboratory, National Institute of Research and Physico-Chemical Analysis, Biotechpole Sidi Thabet 2020, Tunisia

DOI: 10.36348/sjodr.2024.v09i01.003 | **Received:** 26.11.2023 | **Accepted:** 02.01.2024 | **Published:** 17.01.2024

***Corresponding author:** Olfa Zaghden
Oral and Maxillofacial Imaging Resident, Department of Oral Radiology, University Dental Clinic, Monastir University, Monastir, Tunisia

Abstract

This study used CBCT to examine the greater palatine foramen in Tunisian patients, aiming to provide crucial anatomical information for administering greater palatine nerve block anesthesia and identifying appropriate locations for harvesting palatal donor tissue. A total of 63 CBCT scans were conducted on Tunisian patients. All patients had fully erupted first, second, and third molars, leading to the examination of 100 greater palatine foramina (GPF). The evaluation of the GPFs encompassed their positioning, Antero-posterior (AP) and latero-medial (LM) diameters, as well as their distances from both the midline maxillary suture (MMS) and the alveolar ridge top (ART). The measurements were conducted using the distance measuring tool of Romexis® viewer software. The IBM® SPSS® version 20.0 statistical package was used to carry out all statistical analyses. The study included 100 CBCTs, with participants consisting of 37 males (58.73%) and 26 females (41.27%), having an average age of 34±12 years. Among the 100 GPFs analyzed, 68% were near the third molar, 23% were situated behind it, and 9% were positioned opposite to the second molar. The average AP and LM diameters were 4.64mm (±1.15) and 2.53mm (±0.68), respectively. The mean distances to the MMS and ART were 13.9mm (±1.51) and 11.45mm (±2.09), respectively. Among Tunisian patients, the GPF position is quite variable, seldom found opposite to the second molar, and tends to be in closer proximity to the third molar.

Keywords: Greater palatine foramen -Greater palatine canal- Cone beam computed tomography - Maxillary nerve block.

INTRODUCTION

The anesthesia block of the greater palatine nerve (GPN) results in a state of numbness across one side of the upper jaw. This includes the teeth, the mucous membranes of the palate and gums, the skin in the central facial area, the maxillary sinus, and the nasal cavity(Aoun *et al*., 2015).

This technique was first described in 1927(Nevin and Puterbaugh, 1924), and it remains a widely recommended approach for various surgical procedures involving the upper molars, maxillary sinus, and nasal region (Kang *et al*., 2012). Furthermore, it accomplishes nasal hemostasis, a crucial element in multiple procedures such as endoscopic sinus surgery and septorhinoplasty, through the vasoconstrictive impact on the maxillary artery(Schaefer, 2009).

Nonetheless, the anesthesia block can prove ineffective due to the challenge in accurately assessing the greater palatine foramen (GPF) as required(Das *et al*., 2006; Kang *et al*., 2012). In this regard, practitioners commonly utilize a tooth as an indirect reference point to locate the GPF. For instance, they might use the palatal

side of the second molar as a guide for administering anesthesia. Research conducted on dry skulls has indicated that the GPF is typically situated in the vicinity of the second and third molars(Ajmani, n.d.; Chrcanovic and Custódio, 2010; Klosek and Rungruang, 2009; Methathrathip *et al*., 2005; Saralaya and Nayak, 2007; Sharma and Garud, 2013; Sujatha *et al*., 2005). Additionally, in patient cases, a limited number of studies have examined the dimensions of the GPF using both CT scans and endoscopic images(Das *et al*., 2006; Kang *et al*., 2012; Mellema and Tami, 2004). However only three articles in the literature have utilized patient data and cone beam computed tomography (CBCT) images to analyze the position of the GPF(Aoun *et al*., 2015; Ikuta *et al*., 2013; Yilmaz *et al*., 2015)

The variation in the geometry of the GPF are probable due to ethnic variations in craniofacial features, as indicated by previous studies(Ajmani, n.d.; Methathrathip *et al*., 2005; Saralaya and Nayak, 2007). As per the findings of Lorenzo *et al*., the predominant ethnic group among the examined palates was Caucasian, comprising 35.4%, with Indians following at 28.6%, and Asians at 11.1% (Tavelli *et al*., 2019). Nevertheless it is worth noting that few papers that focused on research involving the African population (Ajmani, n.d.; Hassanali and Mwaniki, 1984), and the studies carried out on the Tunisian population are poorly documented.

Therefore, the aim of this study was to assess the GPF location using CBCT images in Tunisian population.

MATERIALS AND METHODS

This study adopts a retrospective approach and involved the examination of 63 archived CBCT scans. These scans included 100 GPF scans sourced from the Medical Imaging Department at the Main Military Training Hospital of Tunis. CBCT scans were obtained and evaluated using a high-resolution medical screen with the Romexis viewer (ProMax 3D Plus®, Planmeca, Finland).

The inclusion criteria encompassed the following conditions:

- Participants aged 18 years or older.
- All upper molars had fully erupted.
- The absence of any pathological conditions or deformities in the jaws was required.

CBCT images of 37 males and 26 females (a total of 100 GPF) met the inclusion criteria and were included in this study.

The images were acquired using the ProMax 3D Plus© device (Planmeca, Finland) which provides a wide range of field of Vue (FOV) between 5 × 5.5 and 23 × 16 cm and voxel sizes of 0.075–0.6 mm (depending on FOV). Images were acquired using 90 kVp and 7 mA, with an exposure time ranging from 3–35 s and a FOV compatible with the recommended indications for referral.

For each GPF scan, four observations were conducted by two observers, both are specialists in oral and maxilla-facial imaging.

1. The GPF's position relative to upper molars.
2. The distance between the GPF and the midline maxillary suture (MMS).
3. The distance between the GPF and the alveolar ridge top (ART).
4. The diameter of the GPF.

The measurements were conducted using the distance measuring tool of Romexis® viewer software and the resulting images were saved in JPEG format.

CBCT Analysis

***The GPF's Position Relative to Upper Molars**

To evaluate the relative position of the GPF concerning the upper molars, two distinct assessment methods were applied.

The first observer adhered to Ikuta *et al*.,'s method (Ikuta *et al*., 2013), involving drawing five tangential lines parallel to the midpoints and interproximal areas of the facial surfaces of the upper molars. These tangents were categorized as follows: (A) From the medial face of the second molar to its center. (B) From the center of the second molar to its distal face. (C) From the medial face of the third molar to its center. (D) From the center of the third molar to its distal face. (E) Distal to the third molar. Subsequently, an axial reconstruction was conducted, revealing an overlap between these drawn tangents and the GPF. This overlap facilitated the assessment of the relationship between the upper molars and the GPF (Figure 1).

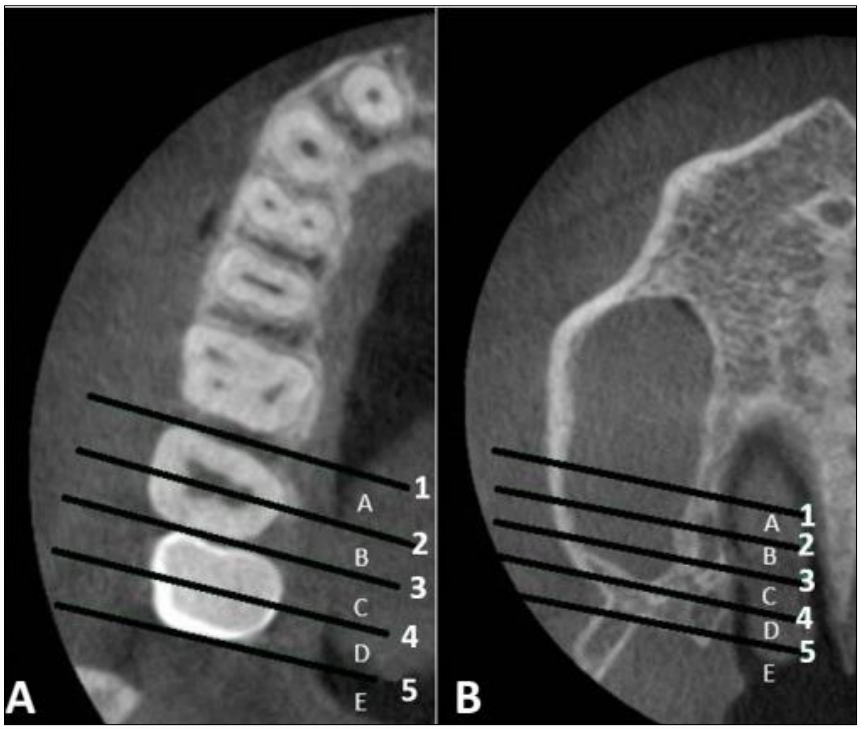

Fig. 1: CBCT: Axial reconstructions were employed to determine the GPF's position in relation to the upper molars. The first axial reconstruction (A) and the subsequent axial reconstruction (b) were used to assess its location

The second observer employed Aoun's method(Aoun *et al*., 2015). Initially, in the sagittal view, the GPF's location was identified. To enhance the visualization of the maxillary molars, the sagittal cut thickness was adjusted to 19.9mm. Using a perpendicular line extended from the GPF location, the GPF's position was classified into one of five positions mentioned above (Figure 2).

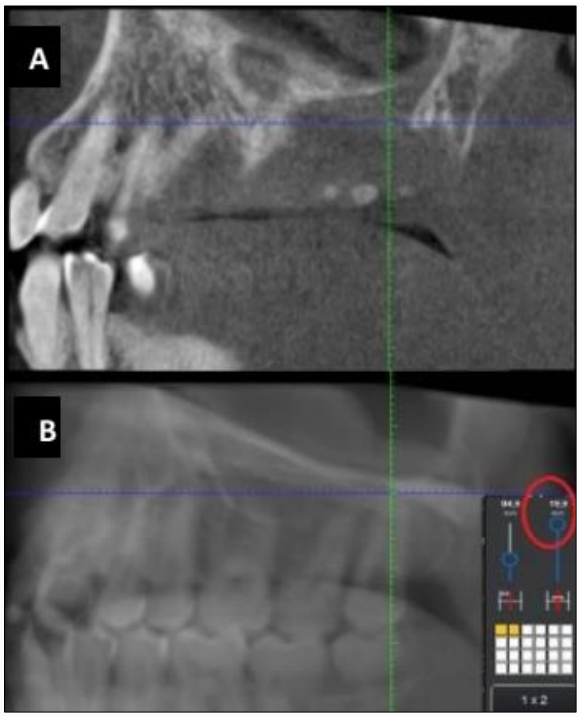

Fig. 2: CBCT: Sagittal reconstructions were employed to determine the GPF's position in relation to the upper molars. The first sagittal reconstruction (A): small thickness cut shows the opening of GPF. The sagittal reconstruction (B): Full thickness (19.9mm: red circle) show the GPF's relative position in relation to the molars

The two sets of results were then compared. In cases where the results did not align, a subsequent examination was conducted by a third observer and the exact position of the GPF has been recorded as a JPEG image.

***Distance between GPF and MMS**

To assess the distance between the GPF and the MMS, a line was drawn from the mesial wall of the GPF to the MMS in the coronal reconstruction (Figure 3).

Fig. 3: CBCT: Coronal reconstruction illustrating the method to determine the distance between GPF and MMS.

***Distance between the GPF and ART**

To quantify the distance separating the GPF and the ART, in the coronal reconstruction, a line was sketched tangentially along the palatal cortex of the maxillary arch, spanning from the ART to the vestibular wall of the GPF (Figure 4).

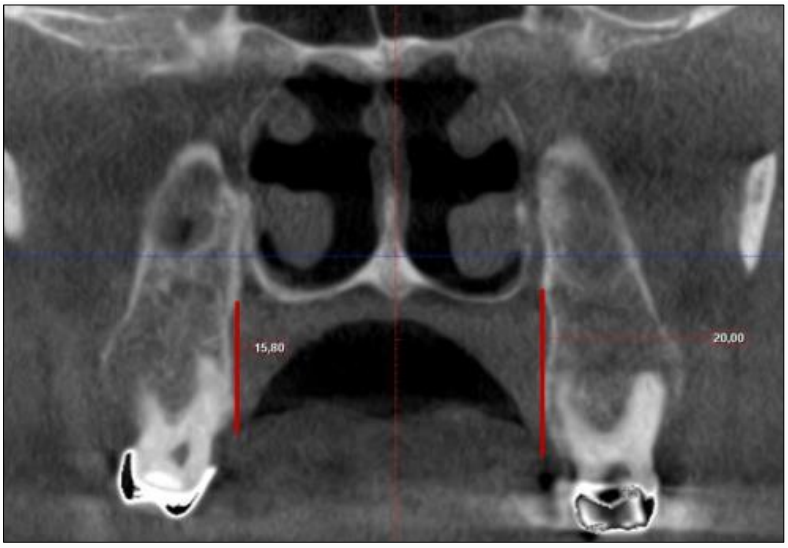

Fig. 4: CBCT: Coronal reconstruction showing how the distance between GPF and ART was determined

***Diameter of GPF**

The average diameter of the GPF was determined using the axial and coronal reconstruction: As the GPF exhibits an oval shape, we opted to assess its main Antero-posterior (AP) and Latero-Medial (LM) axes. (Figure 5).

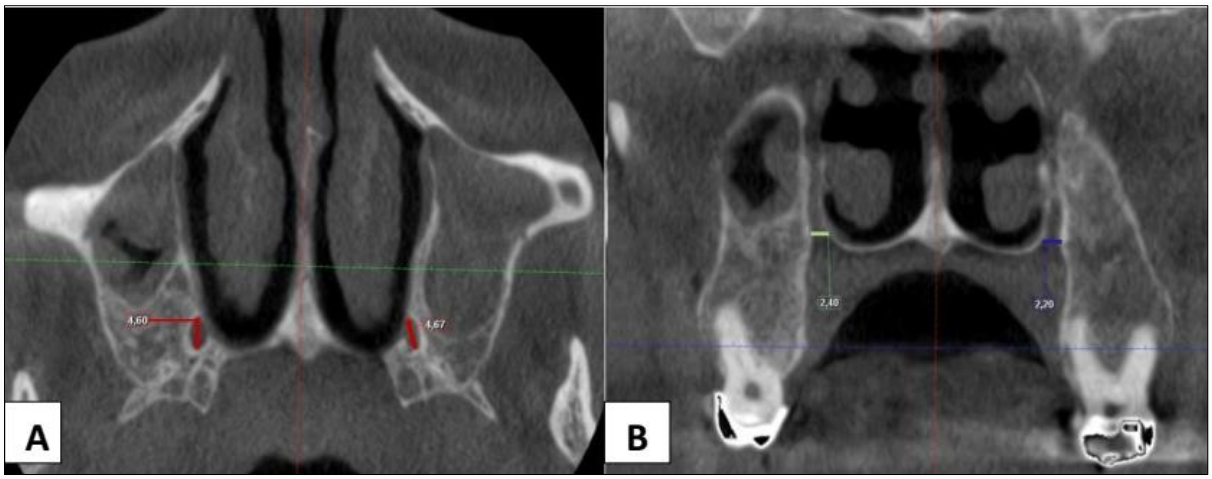

Fig. 5: CBCT: (A) Axial Reconstruction Demonstrating the method for Measuring AP Diameter. (B) Coronal Reconstruction Depicting the Technique Employed to Establish the LM Diameter

Statistical Analysis

Descriptive statistics of age, gender, GPF diameter and location to craniofacial anatomic structures (MMS) and position relative to maxillary molars were calculated. Calculations included determining the mean, standard deviation, minimum, and maximum values for each measurement.

Subsequently, Chi-square test (with a significance level of $P < 0.05$) was executed to compare the measurements between the right and left sides, while the independent T-test was employed to assess the differences in values across genders ($P < 0.05$).

The IBM® SPSS® version 20.0 statistical package was used to carry out all statistical analyses. Statistical significance was set at 0.05. The agreement between examiners was evaluated using Dahlberg's error and subjected to a paired T-test.

RESULTS

A total of 100 CBCTs were included in the study. The research participants comprised 37 males (58.73 %) and 26 females (41.27 %) with a mean age of 34±12 years.

– **Location of the GPF**

Out of the entire set of examinations, the GPF's position was as follows (Table1): 40% were positioned between the center of the third molar and its distal face (position D), 28% were between the medial face of the third molar and its center (position C), 23% were found distal to the third molar (Position E), 5% were situated between the middle of the second molar and its distal face (position B), and 4% were located between the medial face of the second molar and its center (position A).

Table 1: Distribution of GPF location relative to molars

		GPF location relative to molars					Total
		A	B	C	D	E	
GPF_Side	Right side	3	3	14	23	9	52
	Left side	1	2	14	17	14	48
Total		4	5	28	40	23	100

GPF= Greater palatine foramen

– **Distance between GPF and MMS:**

The horizontal distance from the MMS ranged from a minimum of 10,05 mm to a maximum of 17,05 mm with mean distance of 13.9mm (±1.51) (Table 2).

No significant differences were found in measuring the distance between the GPF and the MMS when comparing males and females (p=0.078). Similarly, no statistical significance (p=0.707) was detected when comparing the left and right sides, suggesting that the GPF exhibit symmetry in relation to the MMS.

– **Distance between GPF and ART**

The mean distances from the GPF to the ART was 11.45mm (±2.09) (Table 2).

– **Diameter of GPF**

As for GPF diameter, The AP diameter varied from 1.00 to 7.76 mm with an average of 4.64mm (±1.15) and the LM diameter ranged from 1.32mm to 5.12mm with a mean diameter of 2.53mm (±0,68) (Table 2).

No statistical significance detected in measuring diameters (AP and LM) when comparing right and left side (respectively p=0.3; p= 0.5)

A slight negative correlation was found between the age and both AP and LM diameter (respectively r= -0 .154; -0.068).

Table 2: Descriptive statistics of subjects' age and GPF diameter and location relative to anatomical structures (n=63)

	N	Min.	Max	Mean	SD
Distance to MMS (mm)	100	10,05	17,50	13,9066	1,51483
Distance to ART (mm)	100	6,71	20,00	11,4512	2,09442
Age (years)	63	19,00	66,00	34,8730	12,01141
AP diameter (mm)	100	1,00	7,76	4,6483	1,15683
LM diameter (mm)	100	1,32	5,12	2,5348	,68441
N valide (listwise)	63				

GPF= Greater palatine foramen, MMS= Midline Maxillary Suture, ART= Alveolar ridge top, AP=Antero-posterior, LM= Latero-medial, Max.= Maximum, Min.= Minimum, SD= Standard deviation

DISCUSSION

In our sample of Tunisian adults, we observed considerable variability in the position of the GPF. This variability was evident in the wide spectrum of values and the significant standard deviations found in GPF diameter and its distance from the MMS and ART.

Consistent with the majority of previous studies conducted in different countries, this study reaffirmed that the GPF is most frequently found opposite to the third upper molar (68%) with 40% in position (D) and 28% in position (C) (Ajmani, n.d.; Fu *et al*., 2011; Hassanali and Mwaniki, 1984; Methathrathip *et al*., 2005; Piagkou *et al*., 2012; Saralaya and Nayak, 2007; Sharma and Garud, 2013; Sujatha *et al*., 2005; Tavelli *et al*., 2019). It was also observed that the GPF's position was distal to the third molar in 23% and opposite to the second molar in only 9% of cases. A relatively small number of studies have documented a similar high occurrence of the retromolar position(Chrcanovic and Custódio, 2010; Langenegger *et al*., 1983).Therefore, it appears that the third molar can be considered a reliable landmark when trying to pinpoint the GPF; However it is crucial to consistently conduct palpation of the posterior palate to determine the GPF's location before initiating the anesthesia block of the GPN.

Most research on GPF location has predominantly relied on dry skulls, providing limited information about the age, gender, or ethnicity of the individuals studied. The use of CBCT technology conferred the benefit of assessing patient sex and age, and it also allowed the selection of scans that included all six upper molars to precisely identify the GPF. However, our examination found no variations in GPF location with regard to gender or side and only a small subset of studies provided gender-specific results (Aoun *et al*., 2015; Gibelli *et al*., 2017; Ikuta *et al*., 2013; Langenegger *et al*., 1983; Methathrathip *et al*., 2005; Tomaszewska *et al*., 2014). Thus, it suggests that GPF locations maintain a consistent pattern regardless of sex or side. Furthermore, consistent with a prior study, no disparities were observed when comparing direct measurements in cadavers with the findings from CBCT/CT scans.(Tomaszewska *et al*., 2014)

The examination of anatomical reference points like the ART and the MMS holds significance as they serve as reference markers for identifying the GPF in edentulous patients. Previous studies conducted in Africa has demonstrated that the distances from the GPF to the MMS in dry skulls from Nigeria(Ajmani, n.d.) and south Africa(Langenegger *et al*., 1983) were approximately 15.4mm and 15mm, respectively. These measurements align closely with the findings from our own study which yielded a similar distance of 13.9 mm. In European studies(Nimigean Vanda Roxana, 2013; Piagkou *et al*., 2012; Tomaszewska *et al*., 2014) carried out in Poland, Romania and Greece, the mean distances were reported as 15.8mm , 14.5mm and 15.3mm, respectively. In Asian studies*(Hwang et al*., 2011; Klosek and Rungruang, 2009; Methathrathip *et al*., 2005; Wang *et al*., 1988) the mean distance was approximately 16mm, while several studies on dry skulls from India(Ajmani, n.d.; D'Souza *et al*., 2012; Kumar *et al*., n.d.; Saralaya and Nayak, 2007; Sharma and Garud, 2013; Sujatha *et al*., 2005) reported variable mean distances, ranging from 14.3mm to 16.7mm. Additionally, researches conducted in Brazil (Chrcanovic and Custódio, 2010; Ikuta *et al*., 2013; Urbano *et al*., 2011)showed a significant intra-population variability, with mean distance ranging from14.4 to 16.6mm. These finding highlight notable diversity and differences among different populations.

These results highlight notable diversity and differences among different populations. Despite various studies, there remains a lack of consensus regarding the cause of this variability. Some author propose that this variability may be attributed to ethnic backgrounds(Chrcanovic and Custódio, 2010; Wang *et al*., 1988) while others dispute this theory(Jaffar and Hamada, 2003).

When using the ART as a reference point, we observed that the distance from the ART to the GPF was 11.45mm (±2.09). This point serves various clinical

purposes, including the protection of the palatine nerve during maxillary osteotomy and the establishment of a safety zone to minimize the risk of GPA damage during harvesting procedures. It's important to note that our assessment of the distance from the GPF to the ART cannot be directly compared to other studies, as they typically measure the distance from the GPF to the posterior palate border (Ajmani, n.d.; Chrcanovic and Custódio, 2010; Klosek and Rungruang, 2009; Saralaya and Nayak, 2007)or to the AR(Ikuta *et al*., 2013; Nimigean Vanda Roxana, 2013; Tomaszewska *et al*., 2014), rather than the specific GPF to ART distance, as we have done.

Furthermore, along with establishing the exact GPF location, determining the dimensions of the GPF is essential for the accurate administration of anesthesia. In the current study, the GPF was commonly observed as an oval-shaped opening, a pattern consistent with observations in Thailand(Klosek and Rungruang, 2009; Methathrathip *et al*., 2005) , South Africa(Langenegger *et al*., 1983) and Europe (Nimigean Vanda Roxana, 2013; Piagkou *et al*., 2012; Tomaszewska *et al*., 2014). As indicated by a recent systematic review (Tomaszewska *et al*., 2014)the mean values for the AP and LM diameters of GPF range from 4.5 to 5.3 mm, and 2.2 to 3.25mm, respectively. These measurements align with the findings of our study. A slight negative correlation was found between the age and both AP and LM diameter (respectively r= -0 .154; -0.068). This implies that as individuals grow older, the diameter of the GFP tends to decrease.

This study has limitations. The primary constraint is the small sample size, consisting of only 63 CBCT scans. Additionally, the utilization of CBCTs with varying FOV sizes, chosen based on specific clinical requirements, may have influenced image resolution and, consequently, the obtained results. Nonetheless, the resolution alteration is quite minimal, leading us to the conclusion that it is unlikely to significantly affect the measurements taken. Moreover, our decision to include scans of individuals with all their upper molars erupted, aged 18 years or older, was influenced by the observation made by Savkin *et al*., that the GPF tends to shift towards the posterior as new teeth emerge in children. (Slavkin *et al*., 1966) This choice resulted in the inclusion of a single male individual under the age of 21 (19 years old). Although it is generally accepted that sutural transverse growth of the maxilla ceases around the age of 17 in males(Björk, n.d.; Björk and Skieller, n.d.),studies have indicated that maxillary antero-posterior growth in length continues in males until approximately 20.04 years of age, on average(Nahhas *et al*., 2014).

Despite these constraints, the present study has significantly contributed to providing crucial landmarks for accurately locating the foramen of the greater palatine nerve (FGP). The identification of these landmarks not only enhances the precision of FGP localization but also facilitates the ease with which dentists can successfully perform maxillary anesthesia bloc. This newfound clarity in identifying key anatomical points ensures a more proficient administration of anesthesia, thereby contributing to the maintenance of clinical silence throughout the surgical procedure. The establishment of reliable landmarks is pivotal in optimizing the overall efficacy of maxillary anesthesia, underscoring the importance of this study in advancing the clinical practice of dentistry.

CONCLUSION

The present study provides landmarks for identifying the position of the GPF. We concluded that in the Tunisian patients studied, the GPF location was more closely related to the third molar. Hence, the eruption of the third molar can serve as a reliable landmark for the successful administration of GPN block anesthesia.

Acknowledgements

The authors would like to convey their appreciation to Professor Younes Arous, Head of the Medical Imaging Department at the main military hospital in Tunis, for granting permission to access the CBCT archives for the purpose of this research.

Funding: This research did not receive any specific grant from funding agencies in the public, commercial, or not-for-profit sectors.

Declarations of Interest: none

REFERENCES

- Ajmani, M. L. (1994). Anatomical variation in position of the greater palatine foramen in the adult human skull. *Journal of anatomy*, *184*(Pt 3), 635.
- Aoun, G., Nasseh, I., Sokhn, S., & Saadeh, M. (2015). Analysis of the greater palatine foramen in a Lebanese population using cone-beam computed tomography technology. *Journal of International Society of Preventive & Community Dentistry*, *5*(Suppl 2), S82. https://doi.org/10.4103/2231-0762.171594.
- Björk, A. (1966). Sutural growth of the upper face studied by the implant method. *Acta Odontologica Scandinavica*, *24*(2), 109-127.
- Björk, A., & Skieller, V. (1974). Growth in width of the maxilla studied by the implant method. *Scandinavian journal of plastic and reconstructive surgery*, *8*(1-2), 26-33.
- Chrcanovic, B. R., & Custódio, A. L. (2010). Anatomical variation in the position of the greater palatine foramen. *Journal of oral science*, *52*(1), 109-113. https://doi.org/10.2334/josnusd.52.109.
- D'Souza, A. S., Mamatha, H., & Jyothi, N. (2012). Morphometric analysis of hard palate in south Indian skulls. *Biomed Res*, *23*(2), 173-5.

- Das, S., Kim, D., Cannon, T. Y., Ebert, C. S., & Senior, B. A. (2006). High-resolution computed tomography analysis of the greater palatine canal. *American journal of rhinology*, *20*(6), 603-608. https://doi.org/10.2500/ajr.2006.20.2949.
- Fu, J. H., Hasso, D. G., Yeh, C. Y., Leong, D. J., Chan, H. L., & Wang, H. L. (2011). The accuracy of identifying the greater palatine neurovascular bundle: a cadaver study. *Journal of periodontology*, *82*(7), 1000-1006. https://doi.org/10.1902/jop.2011.100619.
- Gibelli, D., Borlando, A., Dolci, C., Pucciarelli, V., Cattaneo, C., & Sforza, C. (2017). Anatomical characteristics of greater palatine foramen: a novel point of view. *Surgical and Radiologic Anatomy*, *39*, 1359-1368. https://doi.org/10.1007/s00276-017-1899-7.
- Hassanali, J., & Mwaniki, D. (1984). Palatal analysis and osteology of the hard palate of the Kenyan African skulls. *The anatomical record*, *209*(2), 273-280. https://doi.org/10.1002/ar.1092090213.
- Hwang, S. H., Seo, J. H., Joo, Y. H., Kim, B. G., Cho, J. H., & Kang, J. M. (2011). An anatomic study using three-dimensional reconstruction for pterygopalatine fossa infiltration via the greater palatine canal. *Clinical Anatomy*, *24*(5), 576-582. https://doi.org/10.1002/ca.21134.
- Ikuta, C. R. S., Cardoso, C. L., Ferreira-Júnior, O., Lauris, J. R. P., Souza, P. H. C., & Rubira-Bullen, I. R. F. (2013). Position of the greater palatine foramen: an anatomical study through cone beam computed tomography images. *Surgical and Radiologic Anatomy*, *35*, 837-842. https://doi.org/10.1007/s00276-013-1151-z.
- Jaffar, A. A., & Hamadah, H. J. (2003). An analysis of the position of the greater palatine foramen. *J Basic Med Sci*, *3*(1), 24-32.
- Kang, S. H., Byun, I. Y., Kim, J. H., Park, H. K., & Kim, M. K. (2012). Three-dimensional analysis of maxillary anatomic landmarks for greater palatine nerve block anesthesia. *Journal of Craniofacial Surgery*, *23*(3), e199-e202. https://doi.org/10.1097/SCS.0b013e31824de71b.
- Klosek, S. K., & Rungruang, T. (2009). Anatomical study of the greater palatine artery and related structures of the palatal vault: considerations for palate as the subepithelial connective tissue graft donor site. *Surgical and radiologic anatomy*, *31*, 245-250. https://doi.org/10.1007/s00276-008-0432-4
- Kumar, A., Sharma, A., & Singh, P. (2011). Assessment of the relative location of greater palatine foramen in adult Indian skulls: consideration for maxillary nerve block. *Eur J Anat*, *15*(3), 150-154.
- Langenegger, J. J., Lownie, J. F., & Cleaton-Jones, P. E. (1983). The relationship of the greater palatine foramen to the molar teeth and pterygoid hamulus in human skulls. *Journal of dentistry*, *11*(3), 249-256. https://doi.org/10.1016/0300-5712(83)90197-5.
- Mellema, J. W., & Tami, T. A. (2004). An endoscopic study of the greater palatine nerve. *American journal of rhinology*, *18*(2), 99-103. https://doi.org/10.1177/194589240401800206
- Methathrathip, D., Apinhasmit, W., Chompoopong, S., Lertsirithong, A., Ariyawatkul, T., & Sangvichien, S. (2005). Anatomy of greater palatine foramen and canal and pterygopalatine fossa in Thais: considerations for maxillary nerve block. *Surgical and Radiologic Anatomy*, *27*, 511-516. https://doi.org/10.1007/s00276-005-0016-5.
- Nahhas, R. W., Valiathan, M., & Sherwood, R. J. (2014). Variation in timing, duration, intensity, and direction of adolescent growth in the mandible, maxilla, and cranial base: the Fels longitudinal study. *The Anatomical Record*, *297*(7), 1195-1207. https://doi.org/10.1002/ar.22918.
- Nevin, M., Puterbaugh, P. G. (1924). Conduction, Infiltration and General Anesthesia in Dentistry. *Dental Items of Interest Publishing Company*.
- Nimigean, V., Nimigean, V. R., Buţincu, L. A. V. I. N. I. A., Sălăvăstru, D. I., & Podoleanu, L. (2013). Anatomical and clinical considerations regarding the greater palatine foramen. *Rom J Morphol Embryol*, *54*(3 Suppl), 779-783. https://doi.org/10.18231/2455-846X.2017.0004.
- Piagkou, M., Xanthos, T., Anagnostopoulou, S., Demesticha, T., Kotsiomitis, E., Piagkos, G., ... & Johnson, E. O. (2012). Anatomical variation and morphology in the position of the palatine foramina in adult human skulls from Greece. *Journal of Cranio-Maxillofacial Surgery*, *40*(7), e206-e210. https://doi.org/10.1016/j.jcms.2011.10.011.
- Saralaya, V., & Nayak, S. R. (2007). The relative position of the greater palatine foramen in dry Indian skulls. *Singapore medical journal*, *48*(12), 1143.
- Schaefer, S. D. (2009). Endoscopic Sinus Surgery: Anatomy, Three-Dimensional Reconstruction, and Surgical Technique. *Plastic and Reconstructive Surgery*, *124*(2), 658. https://doi.org/10.1097/PRS.0b013e3181b395e8.
- Sharma, N. A., & Garud, R. S. (2013). Greater palatine foramen–key to successful hemimaxillary anaesthesia: a morphometric study and report of a rare aberration. *Singapore Med J*, *54*(3), 152-159. https://doi.org/10.11622/smedj.2013052.
- Slavkin, H. C., Canter, M. R., & Canter, S. R. (1966). An anatomic study of the pterygomaxillary region in the craniums of infants and children. *Oral Surgery, Oral Medicine, Oral Pathology*, *21*(2), 225-235. https://doi.org/10.1016/0030-4220(66)90248-9.
- Sujatha, N., Manjunath, K. Y., & Balasubramanyam, V. (2005). Variations of the location of the greater palatine foramina in dry human skulls. *Indian Journal of Dental Research:*

Official Publication of Indian Society for Dental Research, *16*(3), 99-102.

- Tavelli, L., Barootchi, S., Ravidà, A., Oh, T. J., & Wang, H. L. (2019). What is the safety zone for palatal soft tissue graft harvesting based on the locations of the greater palatine artery and foramen? A systematic review. *Journal of Oral and Maxillofacial Surgery*, *77*(2), 271-e1. https://doi.org/10.1016/j.joms.2018.10.002.
- Tomaszewska, I. M., Tomaszewski, K. A., Kmiotek, E. K., Pena, I. Z., Urbanik, A., Nowakowski, M., & Walocha, J. A. (2014). Anatomical landmarks for the localization of the greater palatine foramen–a study of 1200 head CT s, 150 dry skulls, systematic review of literature and meta-analysis. *Journal of anatomy*, *225*(4), 419-435. https://doi.org/10.1111/joa.12221.
- Urbano, E. S., Melo, K. A., & Costa, S. T. (2011). Morphologic study of the greater palatine canal. *Braz J Morphol Sci*, 102–104.
- Wang, T. M., Kuo, K. J., Shih, C., Ho, L. L., & Liu, J. C. (1988). Assessment of the relative locations of the greater palatine foramen in adult Chinese skulls. *Cells Tissues Organs*, *132*(3), 182-186. https://doi.org/10.1159/000146572.
- Yilmaz, H. G., Boke, F., & Ayali, A. (2015). Cone-beam computed tomography evaluation of the soft tissue thickness and greater palatine foramen location in the palate. *Journal of clinical periodontology*, *42*(5), 458-461. https://doi.org/10.1111/jcpe.12390.